Proceedings Paper:
Robinson, Martin Paul, Zhang, Xiaotian and Flintoft, Ian David (2017) Time Domain Technique for Rapid, Broadband Measurement of Human Absorption Cross Section in a Reverberation Chamber. In: 32nd URSI General Assembly and Scientific Symposium (URSI GASS). , Montreal.

32nd URSI GASS, Montreal, 19-26 August 2017

Time Domain Technique for Rapid, Broadband Measurement of Human Absorption Cross Section in a Reverberation Chamber

Martin P. Robinson, Xiaotian Zhang and Ian D. Flintoft
Department of Electronics, University of York, UK

Abstract

Absorption cross section (ACS) of an object is used in stochastic power balance models, while human ACS is closely related to microwave dosimetry parameters such as specific absorption rate (SAR) and thus characterises exposure as well as effect of human bodies on multipath propagation. ACS, averaged over all directions of incidence, can be obtained in the frequency domain from the S-parameters of two antennas in a stirred-mode reverberation chamber; however, our new time domain method is faster, avoids the need to determine antenna efficiency, and has been validated with a test object of calculable ACS. We can now measure human ACS from 1 to 18GHz, to within 3%, in under 10 minutes. We have done this for 48 subjects, and explored correlations between ACS and body parameters including mass, height, surface area and subcutaneous fat thickness.

1. Introduction

In a reverberant environment, average absorption cross section (ACS) is a useful parameter in power-balance models of propagation, losses and shielding [1, 2]. It characterises an object's response to irradiation from all sides in a multi-path environment, and as the ratio of power losses to incident power density it has dimensions of area.

Average ACS of human bodies is relevant in studies of exposure to microwaves because it is closely related to specific absorption rate (SAR) [3]. It is also useful in communications models, e.g. the effect of passengers on propagation in an aircraft [4, 5]. Broadband measurements of ACS are important because (a) communication systems are moving to higher frequency bands, and (b) they can be related to body composition parameters for medical studies. Penetration of microwaves into body tissue decreases with frequency, so at the lower end of the spectrum the whole body is exposed (and the interaction is correlated with total body water [6]), but at tens of GHz just the body surface [7].

Human ACS measurements need to be made rapidly, owing to the time a subject can maintain a posture, and accurately, to see variations between different people. Here we consider a time domain technique that has advantages over established frequency domain methods.

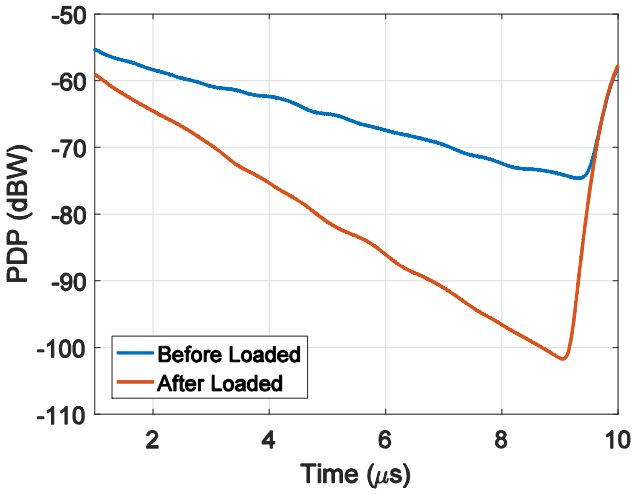

Figure 1. PDP of reverberation chamber showing the increase in τ due to loading with a lossy object. The rise in PDP after 9 μs is an artefact of the IFFT.

2. Measurement of ACS

2.1 Frequency Domain Method

Carlberg et al. [8] show that if the S-parameters of two antennas are measured in a reverberation chamber, total power absorption of the chamber is given by

$$\langle \sigma_{\mathrm{tot}} \rangle = \frac{\lambda^2}{8\pi} \eta_{\mathrm{T}} \eta_{\mathrm{R}} \frac{\left(1 - \left|\langle S_{11} \rangle^2\right|\right)\left(1 - \left|\langle S_{22} \rangle^2\right|\right)}{\left\langle \left|S_{21}\right|^2 \right\rangle} \qquad (1)$$

where λ is wavelength and η_{T}, η_{R} are the efficiencies (thermal losses) of the transmit and receive antennas. Measuring the difference in $\langle\sigma_{\mathrm{tot}}\rangle$ with and without an object present gives that object's ACS, $\langle\sigma_{\mathrm{obj}}\rangle$. The uncertainty in $\langle\sigma_{\mathrm{obj}}\rangle$ depends on the number of independent values of the S-parameters. The range of the technique has been quantified in [9].

2.2 Principle of Time Domain Method

Alternatively, ACS can be found from the time constant τ of the power delay profile (PDP) of the chamber:

$$\left\langle \sigma_{\text{obj}} \right\rangle = \frac{V}{c}\left(\frac{1}{\tau_{\text{wo}}} - \frac{1}{\tau_{\text{no}}} \right) \qquad (2)$$

where V is chamber volume, c speed of light, and subscripts on τ indicate 'with object' and 'no object'. This time domain method is reportedly stabler and more accurate [10], and it also automatically accounts for antenna efficiency.

The PDP comes from an inverse Fourier Transform (IFFT) of the frequency domain data, with a band-limited window [11]. Figure 1 is a typical result showing shorter decay time owing to losses in the object. The rise in PDP at the end of the time window is a consequence of the IFFT which needs to be dealt with.

2.3 Non-linear Fit to Power Delay Profile

Although τ can be found from a simple linear fit to plots such as Figure 1, the result is affected by (a) the shape of window, (b) the selection of range for the fit. Judging the linear part of the PDP by eye leads to errors in ACS of 20 to 30%. To improve on this, we developed a non-linear model that fits to the whole of the time range, and also includes the noise floor of the PDP.

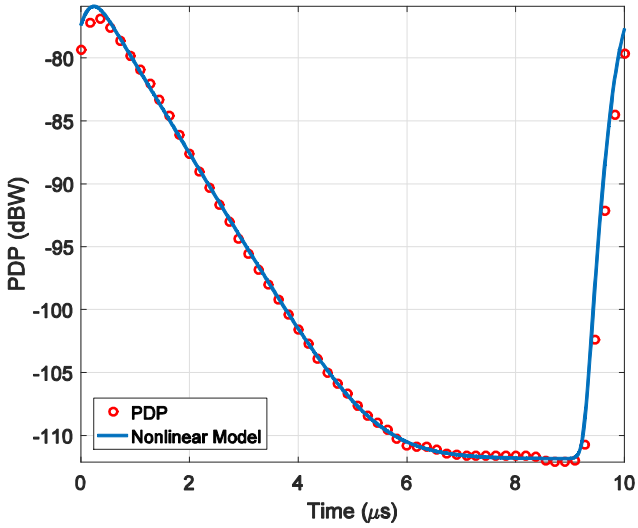

Figure 2. Output of nonlinear model fitted to measured PDP at 10GHz (filtered by a 5MHz smoothed cosine window), showing good agreement with the linear part (0-6 μs), the noise floor (6-9 μs) and the IFFT artefact (9-10 μs).

Figure 2 shows that the algorithm automatically fits to both the noise floor and the IFFT artefact, as well as the linear portion of the PDP.

2.4 Uncertainty of Time Domain Method

A Monte Carlo method was used to evaluate the uncertainty: the algorithm is shown in Figure 3. Measured levels of signal, noise and time constant are combined using Gaussian random processes $N_1(t)$ and $N_2(t)$ and this is repeated N_{idp} times, corresponding to the number of independent measurements in the chamber.

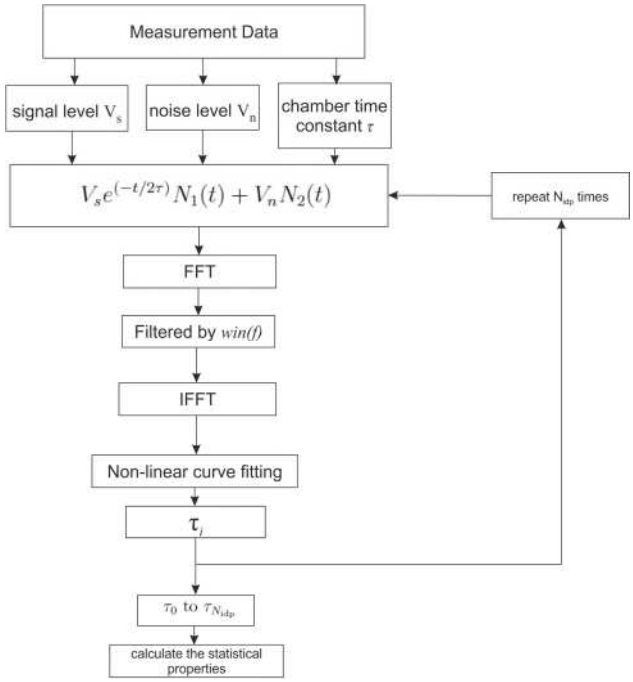

Figure 3. Monte Carlo method for estimating the uncertainty in time-domain measurements of ACS.

Figure 4. Reverberation chamber containing paddle and broadband antennas, loaded with spherical phantom of known ACS.

3. Validation

Validation studies were made with a vector network analyser connected to broadband horn antennas (range 1 to 18GHz) in a reverberation chamber (size 4.7m × 3.0m × 2.37m), fitted with a rotating paddle (Figure 4). To speed up the measurement time, we used a segmented frequency sweep and continuous stirring of the paddle.

The test object was a spherical shell of high density polystyrene, filled with distilled water – both materials of known permittivity and conductivity. Its outer radius was 193.9mm and thickness 3.9mm. ACS was calculated with the Mie series code SPlaC v1.1 [12].

As can be seen in Figure 5, the time domain measurement has less variation than frequency domain, and is closer to the Mie series calculation. This is partly because the former includes the true antenna efficiencies, while the latter assumed an efficiency of 0.95 for each antenna.

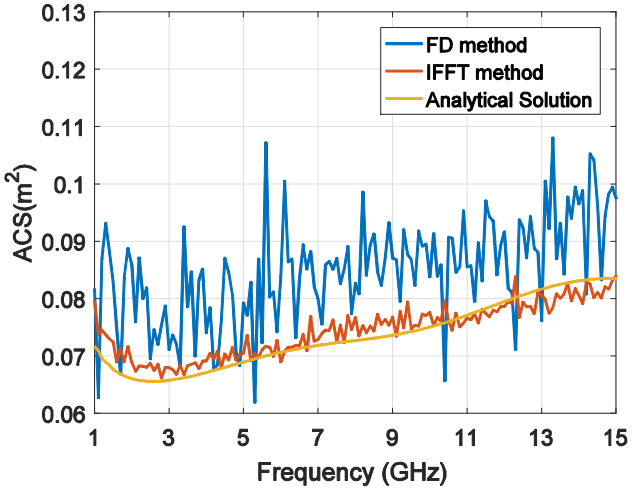

Figure 5. Broadband measurement of ACS of the spherical phantom, using frequency domain and time domain (IFFT) techniques, compared with Mie-series calculation.

Figure 6 shows that the uncertainty in ACS is predicted well by the Monte Carlo model, and is better than 3% for the time domain measurement.

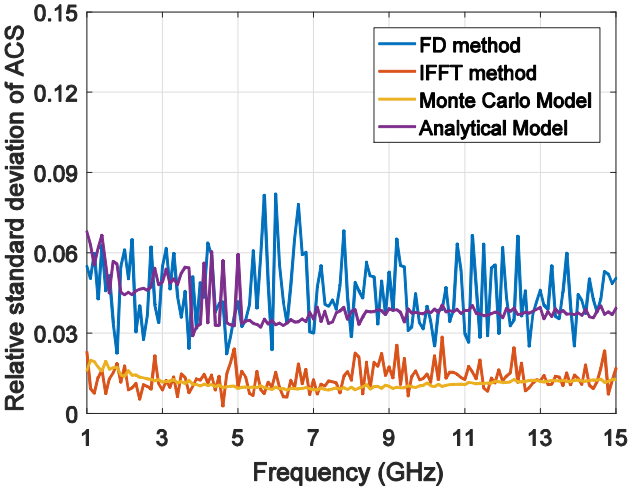

Figure 6. Standard deviation of ACS measurements of the spherical phantom, showing good agreement with the Monte-Carlo model, and lower uncertainty of IFFT compared to frequency domain technique.

4. Human ACS

4.1 Measurement of Human ACS

ACS of 48 subjects was measured with the time domain method. Subjects were asked to lie supine on a block of expanded polystyrene on the chamber floor. Measurement time was 10min.

For all subjects, mass m and height h were also measured. Body fat thickness d_{fat} was estimated from skin fold measurements made with calipers, using the method of Stewart et al. [13]. two sites were chosen at triceps and suprailliac points.

Other parameters were calculated from these measurements. Body mass index (BMI) is h^2/m. Body surface area (BSA) was estimated using the Tikuisis formula [14], and body fat percentage (BFP) from a formula of Gallagher et al. [15].

4.2 Correlation with Body Parameters

Figure 7 shows the results. ACS is similar to previous studies, showing an initial fall and a slower rise from around 7GHz. The apparent outlier with the greatest ACS was actually the heaviest subject.

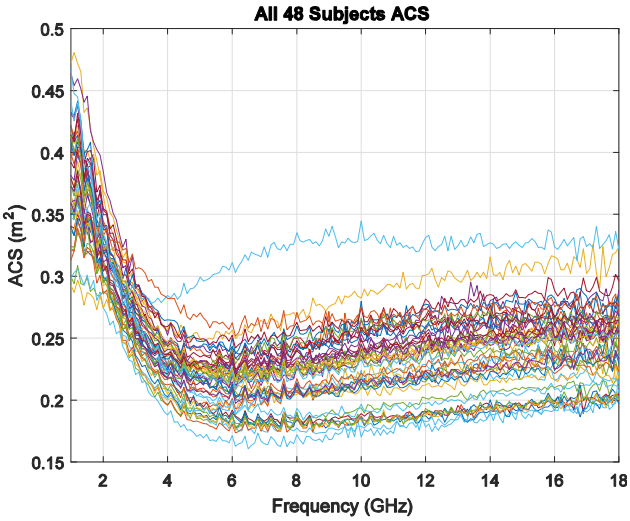

Figure 7. Measured ACS of all 48 subjects.

Figure 8 shows that above 5GHz, the highest correlation is to BSA. Correlation with fat thickness is best at 1GHz. Linear regression (Figure 9) at 1GHz gives

$$\left\langle \sigma_{\text{body}} \right\rangle = 0.0074 d_{\text{fat}} + 0.319 \qquad (3)$$

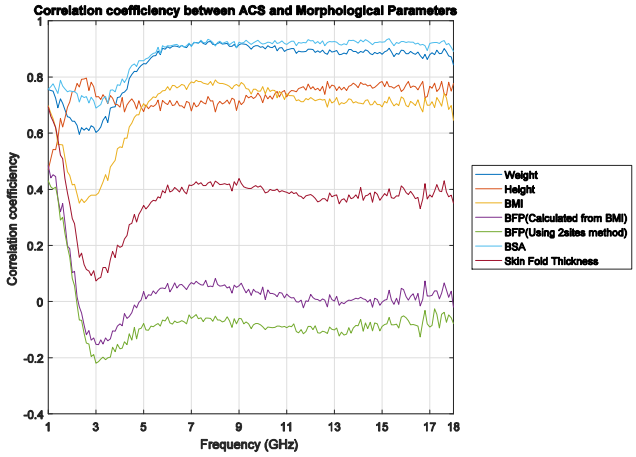

Figure 8. Correlation of ACS with body parameters.

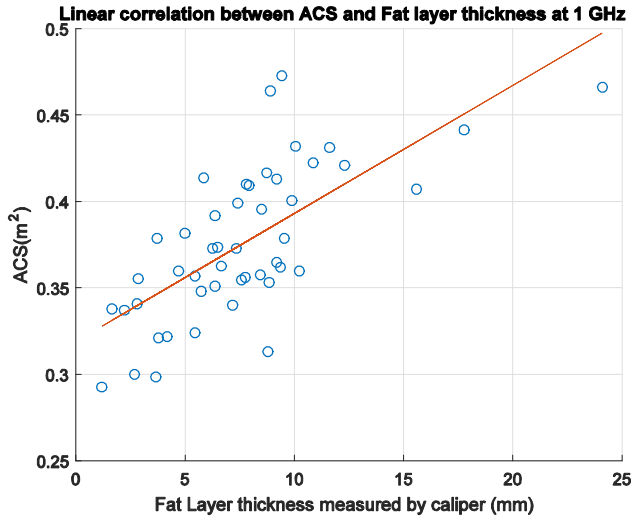

Figure 9. Linear regression of ACS versus fat thickness.

5. Conclusion

The time domain method provides a measurement of ACS that is very broad band – 1 to 18GHz – and takes less than 10min with an uncertainty of better 3%. It is precise enough to study variations between different people, to see how these relate to body composition parameters including fat layer thickness.

6. Acknowledgement

We thank Shane Thurlow for help with the skin fold measurements.

7. References

1. D. Hill, M. T. Ma, A. R. Ondrejka, B. F. Riddle, M. L. Crawford, R. T. Johnk et al., "Aperture excitation of electrically large, lossy cavities," *IEEE Trans. EMC*, **36**, pp. 169–178, 1994.

2. I. D. Flintoft, S. L. Parker, S. J. Bale, A. C. Marvin, J. F. Dawson, and M. P. Robinson, "Measured average absorption cross-sections of printed circuit boards from 2 to 20 GHz," *IEEE Trans. EMC*, **58**, pp. 553–560, 2016.

3. A. Bamba, W. Joseph, J. Andersen, E. Tanghe, G. Vermeeren, D. Plets, J. Nielsen, and L. Martens, "Experimental assessment of specific absorption rate using room electromagnetics," *IEEE Trans. EMC*, **54**, pp. 747–757, 2012.

4. I. D. Flintoft, G. C. R. Melia, M. P. Robinson, J. F. Dawson, A. C. Marvin. 2015, 'Rapid and accurate broadband absorption cross-section measurement of human bodies in a reverberation chamber' *Meas. Sci. Technol.* **26** p. 065701

5. I. D. Flintoft, M. P. Robinson, G. C. R. Melia, A. C. Marvin, J. F. Dawson 2014, 'Average absorption cross-section of the human body measured at 1–12 GHz in a reverberant chamber: results of a human volunteer study' *Phys. Med. Biol.* **59** pp 3297-3317

6. M. P. Robinson, J. Clegg and D. A. Stone 2003. 'A novel method of studying total body water content using a resonant cavity: experiments and numerical simulation' *Phys. Med. Biol.* **48** pp 113-125

7. A. Hirata, Y. Nagaya, F. Osamu, T. Nagaoka, and S. Watanabe, "Correlation between absorption cross section and body surface area of human for far-field exposure at GHz bands," in *EMC 2007. IEEE International Symposium on Electromagnetic Compatibility*, July 2007.

8. U. Carlberg, P.-S. Kildal, A. Wolfgang, O. Sotoudeh, and C. Orlenius, "Calculated and measured absorption cross sections of lossy objects in reverberation chamber," *IEEE Trans. EMC*, **46**, pp. 146–154, 2004.

9. I. D. Flintoft, S. J. Bale, S. L. Parker, A. C. Marvin, J. F. Dawson, and M. P. Robinson, "On the measurable range of absorption cross section in a reverberation chamber," *IEEE Trans. EMC*, **58**, pp. 22–29, 2016.

10. C. L. Holloway, H. A. Shah, R. J. Pirkl, W. F. Young, D. A. Hill, and J. Ladbury, "Reverberation chamber techniques for determining the radiation and total efficiency of antennas," *IEEE Trans. Antennas and Propagation,* **60**, pp. 1758–1770, 2012.

11. X. Zhang, M. P. Robinson, and I. D. Flintoft, "On measurement of reverberation chamber time constant and related curve fitting techniques," in *EMC 2015. IEEE International Symposium on Electromagnetic Compatibility*, Aug 2015, pp. 406–411.

12. E. Le Ru and P. Etchegoin, "SPlaC package v1.1 guide and supplementary information," 2008, http://www.victoria.ac.nz/raman/book/codes.aspx.

13. A. D. Stewart, M. J. Marfell-Jones, J. H. de Ridder. *International Standards for Anthropometric Assessment*, International Society for the Advancement of Kinanthropometry 2006

14. P. Tikuisis P. Meunier, C. Jubenville "Human body surface area: measurement and prediction using three dimensional body scans." Eur. J. Appl. Physiol. **85** pp 264-271, 2001

15. D. Gallagher,et al.. "Healthy percentage body fat ranges: an approach for developing guidelines based on body mass index." Am. J. Clin. Nutrit. **72** pp 694-701, 2000